Journal of Ubiquitous Systems & Pervasive Networks
Volume 17, No. 2 (2022) pp. 67-72

Low Rank Graph Regularization Embedding for 2D+3D Facial Expression Recognition

Yunfang Fu [a, b]*, Yujuan Deng [a, b], Yuekui Zhang [a, b], Zhengyan Yang [a, b], Ruili Qi [a, b]

[a] *School of Computer Science & Engineering, Shijiazhuang University, Shijiazhuang, China, 050035*
[b] *Hebei Province Internet of Things Intelligent Perception and Application Technology Innovation Center, Shijiazhuang, China, 050035*

Abstract

In this paper, a novel low rank graph regularization embedding for 3D facial expression recognition (LRGREFER) approach is proposed, in which the core tensor is utilized to characterize the low-rank attribute among the samples combined with the factor matrices with the graph regularization embedding. At first, a model based on a 4D tensor is constructed from the facial expression data. By Tucker decomposing the constructed 4D tensor, a resulting core tensor and factor matrices in different tensor modes are utilized to characterize the low-rankness among samples. Because of the loss of information during modelling the 4D tensor, the missing data from partly observed facial expression data are recovered by embedding the tensor completion. Finally, the proposed model is handled and solved by adopting the alternating direction method of multipliers (ADMM). Meanwhile, the classification prediction of facial expressions are implemented by Multi-class-SVM. Numerical experiments are conducted on BU-3DFE database. The experiment results have been verified that our proposed approach is more competitive.

Keywords: *Low rank; Graph regularization embedding; Facial expression recognition;Tucker decomposition*

1. Introduction

Expression recognition (FE), which is regarded as an important non-verbal way of human emotional communication and an important branch of automatic face analysis, has attracted more and more attention in the field of computer vision and pattern recognition, and plays an important role in today's scientific challenges.

In last decades, 2D facial expression recognition mainly focuses on 2D modal fusion of images and videos or multi-modal fusion of audio-visual data. Although the 2D FER methods based on face texture analysis have made great progress, they are largely affected by the changes of illumination and pose, which often appear in real scenes.

With the rapid innovation of 3D data acquisition equipment, 3D data are insensitive to variation of illumination and head pose, which are exactly what robust 3D FER requires. Hence 3D FER has wide application prospects in related domains, such as human-computer interface (HCI), pattern recognition, computer vision, image retrieval, facial animation and psychological research [1]. With the BU-3DFE database [2] releasing by the public, researches on 3D Facial expression recognition (3D FER) have attracted enormous attentions [3]. The prototypical expressions include seven basic emotions, i.e. *Disgust (DI)*,*Sadness (SA)*, *Anger (AN), Happiness (HA)*, *Surprise (SU)*, *Fear (FE)* and *Neutral (NE)*, which are widely recognized and keep consistent in different races and cultures.

The approaches based on the model [4] and the feature are regarded as two main streams [4, 5] categorized roughly by existing approaches in 3D FER. Approaches of the former make use of a generic 3D face template firstly, then a number of neutral samples are averaged from this template as the training, and is fitted to match a 3D face as the testing. Finally, the obtained coefficients or parameters from shape deformation in the course of the fitting are finally utilized for subsequent classifier prediction. While the latter often focus on sensitive geometry features of the

*Corresponding author. Tel.:
Fax: ; E-mail: fu_yunfang@126.com

DOI: 10.5383/JUSPN.17.02.003

facial expression from input 3D face scans. The feature-based approaches [3, 5] mainly contain the geometric feature-based, the local patch-based and 2D image mapping-based methods, such as Depth, Texture Map, Gaussian curvature , Shape index features, Mean curvature, Normal Map (NOM), and so on.

The approaches based on the model are attractive theoretically. Due to insufficient recognition features and changes in face mesh topology, they are prone to fatal errors in convergence, e.g. incurred by mouth opening. In addition, they often require high computation. The methods based on the feature are straightforward and often need low computations, while the discriminative power of utilized facial features are depended on substantially, and automatic or manual landmarks are mostly required. In recent years, deep learning based methods [6, 7] and the methods based on tensor decomposition [8, 9] are used and applied into 3D facial expression, and are obtained satisfied results.

However, among the methods above, it is not considered that the low-rank attribute among samples can be characterized by both the factor matrices with the graph regularization embedding and the core tensor. Hence, we propose a low rank graph regularization embedding approach which is applied into 2D+3D facial expression recognition (LRGREFER) in this paper, in which the core tensor is used to characterize the low-rank attribute among the samples combined with the factor matrices with the graph regularization embedding. At the first, a 4D tensor model is constructed from the facial expression data. After Tucker decomposing [10] the constructed 4D tensor, a resulting core tensor and factor matrices in different tensor modes are utilized to characterize the low-rankness among samples. Because of the loss of information in the course of modelling the 4D tensor, the missing data from partly observed facial expression data are recovered by embedding the tensor completion. Finally, the proposed model is handled and solved by using the alternating direction method of multipliers (ADMM). Meanwhile, the classification prediction of facial expressions are implemented by Multi-class-SVM. Numerical experiments are carried out on person-independent and gender-independent cases simultaneously on BU-3DFE database that is the most popularly employed for evaluating 3D FER approaches.

The rest of the paper is organized as follows. Some related preliminaries on tensors are reviewed in Section 2. A novel model based on low rank Tucker decomposition is proposed and solved in Section 3. In Section 4, experiment results are shown. and in Section 5,conclusions are drawn.

2. Preliminaries on Tensors

In this paper, lowercase letters (e.g., y), capital letters (e.g., Y) and calligraphic letters (e.g., $\mathcal{Y}$) represent vectors, matrices and tensors, respectively. Symbols $*$, $\circ$ and $\otimes$ are represented Hadamard product, outer, and the Kronecker , respectively.

2.1. Tucker Decomposition

Tucker decomposition is an effective method to extract the internal structure of multidimensional data. Given an Nth-order tensor $\mathcal{X} \in \mathbb{R}^{I_1 \times I_2 \cdots \times I_N}$ with its elements are represented by $\mathcal{X}_{i_1,i_2,\cdots,i_n}$ $(1 \leq i_n \leq I_n)$, then there always exist integers R_1, $\ldots$, R_n, $\ldots$, R_N $(R_n \leq I_n,\ n = 1, 2 \cdots, N)$, a core tensor $\mathcal{G} = (\mathcal{G}_{r_1 \cdots r_N}) \in \mathbb{R}^{R_1 \times R_2 \ldots \times R_N}$, and matrices $U_1 \in \mathbb{R}^{I_1 \times R_1}$, $\ldots$, $U_N \in \mathbb{R}^{I_N \times R_N}$, so that $\mathcal{X} = \mathcal{G} \times_1 U_1 \times_2 U_2 \cdots \times_N U_N$ when $U_n^T U_n = I_n$ $(n = 1, 2, \cdots, N)$ is satisfied. The Frobenius norm of $\mathcal{X}$ is defined by $\|\mathcal{X}\|_F^2 = \sum_{i_1} \sum_{i_2} \cdots \sum_{i_n} \mathcal{X}_{i_1,i_2,\cdots,i_n}^2$.

In tensor operations, $X_{(n)} \in \mathbb{R}^{I_n \times (I_1 \cdots I_{n-1}, I_{n+1} \cdots I_N)}$ represents the mode-n unfolding of an Nth-order tensor $\mathcal{X}$, where the mode-n folding is the procedure from $X_{(n)}$ to $\mathcal{X}$. The mode-n product of $\mathcal{X}$ with a matrix U_n is denoted by $\mathcal{Y} = \mathcal{X} \times_n U_n$, where $\mathcal{Y} \in \mathbb{R}^{I_1 \times I_2 \times \cdots R_n \times I_{n+1} \cdots \times I_N}$. Meanwhile the mode-$n$ unfolding of $\mathcal{Y} = \mathcal{X} \times_n U_n$ can be represented as $Y_{(n)} = U_n X_{(n)}$.

2.2. Graph regularization Extension

In order to improve the prediction accuracy of multi-dimensional tensor decomposition, the graph regularization framework [11] for tensor factorization is utilized to incorporate sample similarity into matrix factorization, in which the auxiliary information are exploited and regarded as similarity matrices as follows:

$$\begin{aligned} &\min_{\mathcal{G},\{U_n\},\mathcal{X},U_n^T U_n = I_n} \quad \alpha \sum_{n=1}^{N} Tr(U_n^T L_n U_n) \\ &\text{s.t.} \quad \mathcal{X} - \mathcal{G} \prod_{n=1}^{N} \times_n U_n = 0, \mathcal{X}(\Omega) = \mathcal{X}_0(\Omega) \end{aligned} \tag{1}$$

where $\alpha \geq 0$, $Tr(\cdot)$ and $L_n = D_n - W_n$ represent a regulization constant, the matrix trace and the graph Laplacian matrix, respectively. Meanwhile W_n and D_n denote the weight matrix of the samples and the diagonal matrix, i.e., $(D_n)_{ii} = \sum_j (W_n)_{ij}$.

3. The Low Rank Tensor Approach

Now, 3D face scans and 2D face images from a samples are used, in which M kinds of features are extracted with its size of $I_1 \times I_2$ and are constructed into a 4D tensor $\mathcal{X}_0$ with its size of $\mathcal{X}_0 \in \mathbb{R}^{I_1 \times I_2 \times M \times N}$. Because of the information missed in the process of modeling the 4D tensor, an appropriate tensor $\mathcal{X}$ will be utilized by recovering $\mathcal{X}_0$. Meanwhile the orthogonal Tucker decomposition $\mathcal{X} = \mathcal{G} \prod_{n=1}^{4} \times_n U_n$. is used for finding the factor matrices to project the 4D tensor for expression classification prediction.

It is well known that a Tucker decomposition of a high-order tensor has high computational cost, resulting in the ability of solving large-scale problems limited. Motivated by the challenge, we proposed a low rank Tucker decomposition approach for 2D+3D FER by replacing $\|\mathcal{X}\|_*$ with $\|\mathcal{G}\|_*$.

3.1. The Tensor Optimization Model

$Theorem$ 1: Given two tensors: $\mathcal{X} \in \mathbb{R}^{I_1 \times I_2 \times \cdots \times I_N}$ with n-rank = $(r_1, r_2, \cdots, r_N)$, $\mathcal{G} \in \mathbb{R}^{R_1 \times R_2 \times \ldots \times R_N}$ with $R_n \geq r_n$ $(n = 1, 2, \cdots, N)$. If $\mathcal{X} = \mathcal{G} \prod_{n=1}^{N} \times_n U_n$ and $U_n^T U_n = I_{R_n}$ are satisfied , then $\|\mathcal{X}\|_* = \|\mathcal{G}\|_*$ where $\|\mathcal{G}\|_*$ and $\|\mathcal{X}\|_*$ are the trace norm of the core tensor $\mathcal{G}$ and the tensor $\mathcal{X}$, respectively.

According to Theorem 1, the proposed approach is given as the general tensor optimization model in the following:

$$\min_{\mathcal{G},\{U_n\},\{G_{(n)}\}} \quad \sum_{n=1}^{4}\alpha_n\|G_{(n)}\|_* + \gamma\sum_{n=1}^{4}Tr(U_n^T L_n U_n)$$
$$\text{s.t.} \quad \mathcal{X} - \mathcal{G}\prod_{n=1}^{4}\times_n U_n = 0, \mathcal{X}(\Omega) = \mathcal{X}_0(\Omega), U_n^T U_n = I, \quad (2)$$

where γ and α_ns denote a positive tradeoff parameter to compromise the effect of the two terms and the weight of $G_{(n)}$, respectively. The values of the term $\sum_{n=1}^{4}Tr(U_n^T L_n U_n)$ are expected to be small so that discriminatively low dimensional subspace features can be better obtained from the constructed 4D tensor. $\mathcal{X}$ is a recovered and reconstructed tensor. $G_{(n)}$ is the unfolding of the n-mode of $\mathcal{G}$. In order to distinguish $\mathcal{G}$ and $G_{(n)}$, four auxiliary matrices $M_{(n)}$s are introduced into (2) by replacing $G_{(n)}$s, thus (2) is rewritten as:

$$\min_{\mathcal{G},\{U_n\},\{M_n\}} \quad \sum_{n=1}^{4}\alpha_n\|M_n\|_* + \gamma\sum_{n=1}^{4}Tr(U_n^T L_n U_n)$$
$$\text{s.t.}\mathcal{X} - \mathcal{G}\prod_{n=1}^{4}\times_n U_n = 0, G_{(n)} = M_n,$$
$$\mathcal{X}(\Omega) = \mathcal{X}_0(\Omega), U_n^T U_n = I, \quad (3)$$

3.2. Solution of the Optimization Problem

Obviously, problem (3) is nonlinear and non-convex including lots of constraints and variables. To solve this problem and ease the computation, the alternating direction method of multipliers (ADMM) [12] is utilized. Now, the augmented Lagrange function of (3)is defined as below by being given $(\mathcal{G}, \{U_n\}, \mathcal{X}, \{M_n\}, \mathcal{P}^x, \{P_n\}, \mathcal{P}_t, \mu)$:

$$\begin{aligned}
&\mathfrak{L}_\mu(\mathcal{G}, \{U_n\}, \{M_n\}, \mathcal{P}_x, \{P_n\}, \mathcal{P}_t)\\
&= \sum_{n=1}^{4}\alpha_n\|M_n\|_* + \gamma\sum_{n=1}^{4}Tr(U_n^T L_n U_n)\\
&+ < \mathcal{X} - \mathcal{G}\prod_{n=1}^{4}\times_n U_n, \mathcal{P}_x > + \frac{\mu}{2}\|\mathcal{X} - \mathcal{G}\prod_{n=1}^{4}\times_n U_n\|_F^2\\
&+ \sum_{n=1}^{4} < G_{(n)} - M_n, P_n > + \frac{\mu}{2}\sum_{n=1}^{4}\|G_{(n)} - M_n\|_F^2\\
&+ < \mathcal{X}(\Omega) - \mathcal{X}_0(\Omega), \mathcal{P}_t > + \frac{\mu}{2}\|\mathcal{X}(\Omega) - \mathcal{X}_0(\Omega)\|_F^2, \quad (4)
\end{aligned}$$

where $\mu > 0$ is a scalar, U_n must satisfy $U_n^T U_n = I_n$ ($n = 1, 2, 3, 4,$), $\mathcal{P}_x$, $P_n s$ and $\mathcal{P}_t$ are the Lagrange multipliers,.

3.2.1. Solution of $\mathcal{G}$

By fixing other parameters, $\mathcal{G}$ can be solved by :

$$\min_{\mathcal{G}} \quad \frac{\mu}{2}\|\mathcal{G} - \mathcal{Q}\|_F^2 + \frac{\mu}{2}\sum_{n=1}^{4}\|G_{(n)} - M_n + \frac{P_n}{\mu}\|_F^2. \quad (5)$$

where $\mathcal{Q} = (\mathcal{X} + \frac{\mathcal{P}_x}{\mu})\prod_{n=1}^{4}\times_n U_n^T$, a closed-form solution can be given:

$$\mathcal{G} = \frac{\mu(\mathcal{Q} + \mathcal{N})}{\mu(N+1)} \quad (6)$$

where $\mathcal{N} = \sum_{n=1}^{4} fold(M_n - P_n)$ and $N = 4$.

3.2.2. Solution of U_n's

By fixing $U_k(k \neq n)$ and other parameters, $U_n(1 \leq n \leq 4)$ can be updated by

$$\min_{U_n^T U_n = I} \frac{\mu}{2}\|\mathcal{X} - \mathcal{G}\prod_{n=1}^{4}\times_n U_n + \frac{\mathcal{P}_x}{\mu}\|_F^2 + \gamma Tr(U_n^T L_n U_n) \quad (7)$$

Utilizing the equation $\mathcal{Y} = \mathcal{S}\times_n V \Leftrightarrow Y_{(n)} = V S_{(n)}$, (7) turns to the problem as below:

$$\max_{U_n^T U_n = I} < U_n, A_n > . \quad (8)$$

where $A_n = \mu(\mathcal{X} + \frac{\mathcal{P}_x}{\mu})_{(n)}\mathcal{G}_{(-n)}^T - \gamma L_n U_n$,and $\mathcal{G}_{(-n)} = \mathcal{G}\prod_{k=1,k\neq n}^{4}\times_k U_k^T$. (8) can be solved easily by using the $von\ Neumann$'s $trace\ inequality$ [13] by

$$U_n = B_n C_n, \quad (9)$$

where $A_n = B_n D_n C_n$ is the SVD decomposition of A_n.

3.2.3. Solution of $\mathcal{M}_n$'s

By fixing $M_k(k \neq n)$ and other parameters, $\mathcal{M}_n(1 \leq n \leq 4)$ can be updated by

$$\min_{\mathcal{M}_n} \alpha_n\|M_n\|_* + \frac{\mu}{2}\|G_{(n)} - M_n + \frac{P_n}{\mu}\|_F^2. \quad (10)$$

Hence, a closed-form solution is achieved in (10) as follows:

$$M_n = \Theta_{\frac{\alpha_n}{\mu}}(G_{(n)} + \frac{P_n}{\mu}) \quad (11)$$

where $\Theta_\delta(W) = DS_\delta(\Sigma)V^T$, in which the singular value decomposition (SVD) of any matrix W denotes $W = D\Sigma V^T$, and $S_\delta(\Sigma_{ij})$= $\max(0, \Sigma_{ij} - \delta)$ represents the soft-thresholding operator.

3.2.4. Solution of $\mathcal{X}$

By fixing other parameters, $\mathcal{X}$ is be achieved easily to implement with the following method:

$$\begin{cases} \overline{\Omega}(\mathcal{X}) = \overline{\Omega}(\mathcal{G}\prod_{n=1}^{4}\times_n U_n - \frac{\mathcal{P}_x}{\mu}), \\ \Omega(\mathcal{X}) = \Omega(\mathcal{G}\prod_{n=1}^{4}\times_n U_n - \frac{\mathcal{P}_x}{\mu} + \mathcal{X}_0 - \frac{\mathcal{P}_t}{\mu}). \end{cases} \quad (12)$$

The proposed algorithm can be summarized combined with the ADMM framework in Algorithm 1.

Algorithm 1 Solving Problem (3) by ADMM

Input: A tensor $\mathcal{X}_0 \in \mathbb{R}^{I_1 \times I_2 \ldots \times I_4}$; Parameters $\alpha_n, \gamma, t_{max}$;
Output: Factor matrices $\{U_n\}_{n=1}^4$;

Step 0 Initialization: choose $\{U_n^0\}_{n=1}^4, \mathcal{G}^0, \mathcal{X}^0, \rho, \mu^0, \{M_n^0\}_{n=1}^4$ and set $t = 0$;
Step 1 Update $\mathcal{G}^t$ by (6);
Step 2 Update $\{U_n^t\}_{n=1}^4$ by (9);
Step 3 Update $\mathcal{X}^t$ by (12);
Step 4 Update M_n^t by (11);
Step 5 Update multipliers by $\mathcal{P}_x^t = \mathcal{P}_x^{t-1} + \mu^{t-1}(\mathcal{X}^t - \mathcal{G}^t \prod_{n=1}^4 \times_n U_n^t)$, $P_n^t = P_n^{t-1} + \mu^{t-1}(G_{(n)}^t - M_n^t)$ and $\mathcal{P}_t^t = \mathcal{P}_t^{t-1} + \mu^{t-1}(\mathcal{X}^t(\Omega) - \mathcal{X}_0(\Omega))$;
Step 6 Let $\mu^t = \rho\mu^{t-1}$;
Step 7 t=t+1; While some stop criteria are not satisfied, go to Step 1.

4. Experiment Results

Experiments are implemented in the BU-3DFE database. BU-3DFE database consists of 56 femals and 44 males with various ethnic backgrounds, ranging age from 18 years to 70 years old and including East-Asian, White, Middle-east Asian, Black, Hispanic Latino and Indian. The expressions include a neutral expression and six prototypic expressions (see Fig.1) with four intensity levels ranging from 1 to 4. 90% of 100 subjects are selected randomly regarded as the training, while the rest as the testing, and we repeat the experiments for 10 times and treat Multi-Class-SVM as the classifier in all experiments.

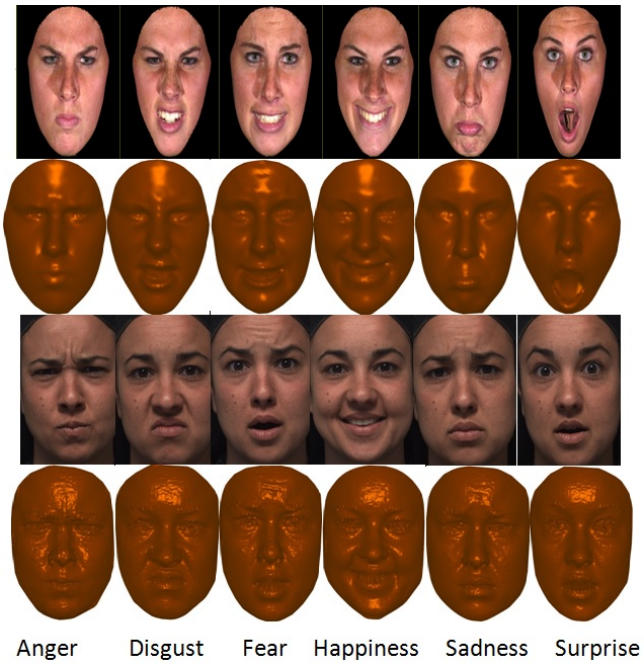

Fig. 1. Visualization of six basic expressions with face images and facial models in BU-3DFE database.

4.1. Experimetal Details

Three parts are discussed in this subsection: the first one is the nine features extracted, the second is the parameters in Algorithm1, and the last one is the stopping criterion. The nine features are extracted firstly by 2D maps, and then processed by LBP descriptor [14] which is widely used in 2D and 3D fields, the details can be seen in [8]. And the extracted nine features are depth map I_g, 3-channel textured maps I_t^r, I_t^g and I_t^b which can be introduced in [15], 3-direction normal maps I_n^x, I_n^y and I_n^z, and curvature maps I_c (curvature) and I_{mc} (mean curvature). Fig. 2 shows the nine types of features of 2D maps and 2D texture information of four 3D face scans with four intensity level in BU-3DFE database.

Fig. 2. Illustration of happiness expressions of four 3D face scans with nine kinds of extracted features in BU-EDFE database. And from left to right are the depth maps, 3-channel textured information (R, G, B), 3-direction normal maps (x, y, z), and curvature maps (curvature and mean curvature).

The parameters in the experiments are set as below: $\alpha_n (n = 1, 2, 3, 4)$ are set to be 0.1, 0.1, 10,0.01, respectively, and γ is set to be 100, and ζ is set to be 1e-4 in the experiments.

In Algorithm 1, the stop criteria can be set by

$$\|\Omega(\mathcal{X}^{[t]} - \mathcal{G}^{[t-1]} \prod_{n=1}^{4} \times_n U_n^{[t-1]})\|_F / \|\mathcal{X}_0\|_F < \zeta,$$

with some sufficiently small $\zeta > 0$, or the iteration process will be terminated when $t > t_{\max}$.

4.2. Experimental Evaluation

In this subsection, we evaluate our proposed approach in three parts: the average confusion matrix of six expressions, the convergence behavior of our proposed approach, and comparison results with other state-of-the-art methods. The first part are given in Table 1. It is found obviously that happiness and surprise expressions can be easily recognized because of their high facial muscle deformation, while the recognition of disgust and fear are obtained are more difficult. Meanwhile, it is easily found that fear can be confused with other any expressions.

Table 1. Average Confusion Matrix of six expressions on BU-3DFE for 10 Times.

%	AN	DI	FE	HA	SA	SU
AN	**96.42**	1.15	0.65	0.00	1.78	0.00
DI	2.71	**92.13**	3.53	0.42	0.00	1.21
FE	0.32	1.63	**89.35**	6.36	1.50	0.84
HA	0.00	0.05	1.04	**98.91**	0.00	0.00
SA	2.46	0.91	1.87	0.00	**94.76**	0.00
SU	0.00	0.49	0.21	0.42	0.00	**99.30**
Accuracy(%)	**95.15**					

The convergence behavior is shown in Fig. 3 by using the log relative error $\log_{10}$(RE), where RE $:= \|\mathcal{X}^{[k+1]} - \mathcal{X}^{[k]}\|_F / \|\mathcal{X}\|_F$ with $\mathcal{X}^{[k]} := \mathcal{G}^{[k]} \prod_{n=1}^{4} \times_n U_n^{[k]}$. From Fig. 3, it is easily observed that our approach requires less iterations and generates a non-increasing sequence of objective values, which shows the advantage of our proposed approach via the low-rankness graph regularization embedding.

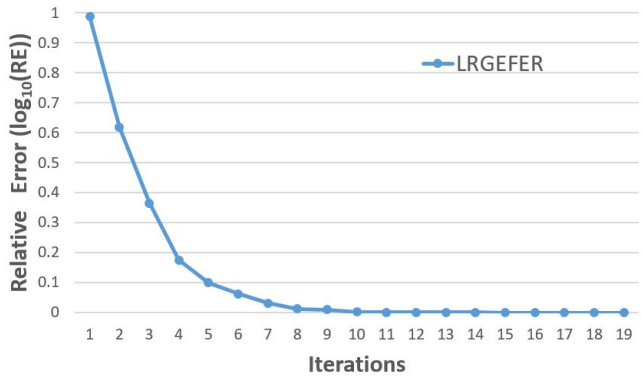

Fig. 3. The convergence behavior in BU-3DFE database.

At the same time, some state-of-the-art methods are compared with our proposed approach, the comparisons are given in Table 2. From this table, it is found the state-of-the-art methods [16–18] that used vector features do not outperform our proposed approach because vector features do not maintain the structral information. Meanwhile the method [5], which constructs a 4D tensor model to explore the intrinsic strucutral information and corelations among multi-mode data from 2D images and 3D scans for the first time, do not consider low-rankness atribute among 3D scan samples, resulting in its recognition result is not better than that of our proposed approach. Thus, our proposed approach are more competitive from Table 2.

Table 2. The comparisons with the state-of-the-art methods.

Method	Accuracy
Soyel et al. [16]	95.10
Wang et al.[17]	83.60
Zhao et al. [18]	82.30
Fu et al.[5]	85.802
Ours	**95.15**

5. Conclusions

In this paper, we have proposed a low rank model with graph regularization embedding and applied into 2D+3D facial expression recognition (LRGREFER). At first, a 4D tensor is built by extracting nine kinds of features from 2D face images and 3D face scans. Secondly, low rank attribute of 4D tensor among samples is characterized by a core tensor and four factor matrices by Tucker decomposing the 4D tensor. Thirdly, a tensor completion framework is embedded because of the data missed in the course of the 4D tensor modelling. Finally, the ADMM algorithm is utilized to solve the proposed optimization model. The numerical experiments have been verified that the proposed approach is more competitive. In the future, more effective low rank algorithms based on Tucker decomposition are required, which is one topic of our future research.

Acknowledgments

This work was partly supported by the National Natural Science Foundation of China (61471032), Hebei Province Internet of Things Intelligent Perception and Application Technology Innovation Center, and Innovation Capability Improvement Plan Project of Hebei Science and Technology Department(21557611K), and Doctoral Research Foundation of Shijiazhuang University(21BS018).

References

[1] Tianhong Fang, Xi Zhao, Omar Ocegueda, Shishir K. Shah, and Ioannis A. Kakadiaris. 3D/4D facial expression analysis: An advanced annotated face model approach. *Image Vis. Comput.*, 30(10):738–749, 2012.

[2] Lijun Yin, Xiaozhou Wei, Yi Sun, Jun Wang, and Matthew J. Rosato. A 3D facial expression database for facial behavior research. In *Int. Conf. Automat. Face Gesture Recog.*, pages 211–216, 2006.

[3] C. A. Corneanu, M Oliu, J. F. Cohn, and S Escalera. Survey on rgb, 3D, thermal, and multimodal approaches for facial expression recognition: History, trends, and affect-related applications. *IEEE Trans. Pattern Anal. Mach. Intell.*, 38 (8):1548–1568, 2016.

[4] Qingkai Zhen, Di Huang, Yunhong Wang, and Liming Chen. Muscular movement model-based automatic 3D/4D facial expression recognition. *IEEE Trans. Multimedia*, 18 (7):1438–1450, 2016.

[5] Yunfang Fu, Qiuqi Ruan, Gaoyun An, and Yi Jin. Fast nonnegative tensor factorization based on graph-preserving for 3D facial expression recognition. In *IEEE Int. Conf. Signal Process.*, pages 292–297, 2017.

[6] Z. Chen, H. Di, Y. Wang, and L. Chen. Fast and light manifold cnn based 3D facial expression recognition across pose variations. In *2018 ACM Multimedia Conference*, pages 229–238, 2018.

[7] I. H. Trimech, A. Maalej, and Neb Amara. Data augmentation using non-rigid cpd registration for 3D facial expression recognition. In *2019 16th International Multi-Conference on Systems, Signals and Devices (SSD)*, pages

164–169, 2019.

[8] Y. Fu, Q. Ruan, Z. Luo, Y. Jin, G. An, and J. Wan. Ferlrtc: 2D+3D facial expression recognition via low-rank tensor completion. *Signal Processing*, 161:74–88, 2019.

[9] Y. Fu, Q. Ruan, and Y. Jiang. Sparse and lowrank tucker decomposition with its application to 2D+3D facial expression recognition. In *2020 15th IEEE International Conference on Signal Processing (ICSP)*, pages 37–42, 2020.

[10] Tamara G. Kolda and Brett W. Bader. Tensor decompositions and applications. *SIAM Rev.*, 51(3):455–500, 2009.

[11] Y. Liu, F. Shang, W. Fan, J. Cheng, and H. Cheng. Generalized higher order orthogonal iteration for tensor learning and decomposition. *IEEE Trans. Neural Netw. Learn. Syst.*, PP(99):1–13, 2015.

[12] Stephen Boyd, Neal Parikh, Eric Chu, Borja Peleato, and Jonathan Eckstein. Distributed optimization and statistical learning via the alternating direction method of multipliers. *Found. Trends® Mach. Learn.*, 3(1):1–122, 2011.

[13] L. Mirsky. A trace inequality of john von neumann. *Monatshefte Für Mathematik*, 79(4):303–306, 1975.

[14] Caifeng Shan, Shaogang Gong, and Peter W. Mcowan. Facial expression recognition based on local binary patterns: A comprehensive study. *Image Vis. Comput.*, 27(6): 803–816, 2009.

[15] Huibin Li, Jian Sun, Zongben Xu, and Liming Chen. Multimodal 2D+3D facial expression recognition with deep fusion convolutional neural network. *IEEE Trans. Multimedia*, PP(99):1–1, 2017.

[16] Hamit Soyel and Hasan Demirel. Facial expression recognition using 3D facial feature distances. In *Int. Conf. Image Anal. Recog.*, pages 831–838, 2007.

[17] Jun Wang, Lijun Yin, Xiaozhou Wei, and Yi Sun. 3D facial expression recognition based on primitive surface feature distribution. In *Proc. IEEE Conf. Comput. Vis. Pattern Recog.*, volume 2, pages 1399–1406, 2006.

[18] Xi Zhao, Di Huang, Emmanuel Dellandrea, and Liming Chen. Automatic 3D facial expression recognition based on a bayesian belief net and a statistical facial feature model. In *Int. Conf. Pattern Recog.*, pages 3724–3727, 2010.